

Self-Soldering Connectors for Modular Robots

Jonas Neubert, *Member, IEEE*, Arne Rost, *Member, IEEE*, and Hod Lipson, *Member, IEEE*

Abstract—The connection mechanism between neighboring modules is the most critical sub-system of each module in a modular robot. Here we describe a strong, lightweight, solid state connection method based on heating a low melting point alloy to form reversible soldered connections. No external manipulation is required for forming or breaking connections between adjacent connectors, making this method suitable for reconfigurable systems such as self-reconfiguring modular robots. Energy is only consumed when switching connectivity, and the ability to transfer power and signal through the connector is inherent to the method. Soldering connectors have no moving parts, are orders of magnitude lighter than other connectors, and are readily mass manufacturable. The mechanical strength of the connector is measured as 173 N, enough to support many robot modules, and hundreds of connection cycles are performed before failure.

Index Terms—Cellular and Modular Robots; Self-reconfiguration; Connectors

I. INTRODUCTION

Modular robots are machines consisting of a collection of independent self-contained smaller machines of identical or similar type. A subset of modular robots has the property of self-reconfigurability, meaning that, through appropriate actuation, the robot can change the arrangement of its own modules without external manipulation. Self-reconfiguration implies that physical connections between modules must be formed and broken over time. Therefore, a reversible connection method is required, and each module must have full control over the connections to its neighbors.

The method applied to form a connection between the modules of a modular robot is widely recognized as key design element of any such system [1]–[7]. Mechanical properties such as tensile strength restrict the space of possible module configurations. Reversibility and repeatability define the scope of possible reconfiguration operations. Electrical properties of the connection mechanism place constraints on the power distribution and communication between modules.

Most existing connectors for self-reconfiguring modular robots add significant complexity to each module. The majority of connection methods reported in literature rely on mechanical actuation for the connection or disconnection process, or both. For a cube shaped module, for example, this requires either six separate actuators or a complex transmission mechanism for actuating connectors on all six faces.

Manuscript received January 23, 2014; revised June 21, 2014. This work was supported by the U.S. National Science Foundations Office of Emerging Frontiers in Research and Innovation, grant #0735953.

J. Neubert and H. Lipson are with the Creative Machines Lab, Cornell University, Ithaca, NY, 14853 USA. h1274@cornell.edu jn283@cornell.edu

A. Rost is with Festo AG & Co. KG, 73734 Esslingen, Germany rost@de.festo.com

This paper has supplementary downloadable material available at <http://ieeexplore.ieee.org>

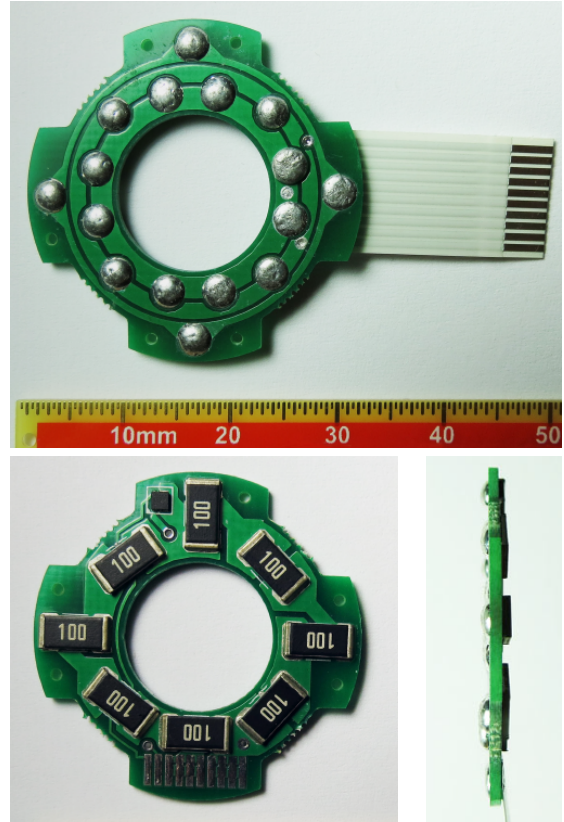


Fig. 1. The self-soldering connector. The outward facing side of the connector printed circuit board (top) contains pads covered with low melting point solder. Opposite (bottom left) resistors act as heater to melt the solder during connection and disconnection operations. The connector weighs only 2 g, is less than 3 mm thick, is readily mass manufactured and can be easily customized to integrate in self-reconfiguring robot systems of various shapes and scales.

In addition to adding volume, weight, and part cost, the assembly of mechanisms complicates the manufacturing of modules. The latter point in particular is an obstacle towards realizing the three oft-cited promises of modular robotics: versatility, robustness, and low cost [4], [5], [8]. To realize this potential, modules must be produced reliably and cheaply in large quantities.

In this paper we present a connector that has no moving parts, weighs orders of magnitude less than comparable mechanical connectors, and is easily mass-produced (Fig. 1). When used in conjunction with similarly scalable manufacturing processes for other components of the module, this might pave the way towards the construction of a self-reconfiguring modular robot system with hundreds of modules, as would be required to realize the benefits of modular robot systems at a scale beyond prototype demonstrations.

II. REQUIREMENTS

In literature, there is broad agreement on the desirable properties of connectors in modular robotic systems [2], [9], [10]:

a) Size: Because each module contains multiple instances of the connector, connector size is one of the primary drivers of overall module size. Scalability considerations and actuator torque characteristics generally favor small module sizes, making small connectors desirable.

b) Mechanical Strength: With the primary purpose of a connector being to connect many modules physically to form a larger system, the mechanical strength of the weakest module-to-module connection can define the strength of the overall system. Connectors must function under all loading scenarios encountered during the operation of the modular robot, which might include carrying the load of other modules.

c) Information Transmission Capability: For a robot to autonomously self-reconfigure, information must be shared among the modules without an external intermediary. Transferring information through the connector is often more favorable than wireless techniques, especially in large systems or when local communication between neighbors only is the primary type of communication in the structure.

d) Power Transmission Capability: Sharing of power across modules can be beneficial in systems where only some modules store energy, or to lessen the momentary demands on batteries during local high current consumption.

e) Reversibility and Repeatability: Self-reconfiguration requires that connections cannot only be formed but also broken. Multiple connection-disconnection cycles must be possible to support even basic reconfiguration scenarios.

f) Speed of (Dis-)connection: Non-trivial reconfiguration tasks may frequently require sequences of connection and disconnection steps. Fast (dis-)connection operations are therefore desirable to keep the overall duration of reconfiguration tasks short. This equally applies to systems where reconfiguration is employed for locomotion (e.g. [11], [12]) and robot speed is inversely proportional to (dis-)connection time.

g) Tolerance to Misalignment: Sources of error in positioning and alignment of modules are manifold. In modular robot design a tradeoff exists between engineering a system where module position and orientation is precise, and a system that tolerates misalignment. Because positioning and orientation errors accumulate in chain and lattice configurations, systems intended to scale to large numbers of modules should not rely on connectors that tolerate mis-alignment because this approach limits the overall size of the system. Nevertheless, it is desirable for the connection mechanism to tolerate some amount of misalignment.

h) Power Consumption: Energy and power availability in each module is limited. When power is distributed between modules, current and power ratings of internal components are the limiting factor. Without power distribution, capacity and power rating of the battery place limits on total and peak power consumption, respectively.

i) Genderlessness and Orientation-invariance: Gendered and orientation-dependent connectors reduce the number of

possible configurations of a modular robot system. For example, if the connectors of cube shaped modules in a lattice-type system have no rotational symmetry, two modules can only be connected in six distinct configurations. In contrast, a four-way rotationally symmetric connector is effectively orientation-invariant because it allows for connecting two modules in all 24 configurations in which both modules are aligned with the lattice. Therefore, it is desirable for the connectors to be genderless and exhibit rotational symmetries.

j) Unilateral Actuation: Connectors that can be unilaterally (dis-)connected allow for continued operation when a neighboring module fails, the existence of passive modules in the system, and for control of module assembly behaviors without synchronization between modules. While not strictly required for a self-reconfiguring modular system, this improves reliability and versatility of the modular robot. [13]

A variety of approaches towards meeting all or a large subset of these requirements have been presented in literature, a review of which is provided in Section VI. The connector presented in this paper uses a metallic binder material between adjacent modules' connectors. The connectors themselves generate heat to melt the binder material during connection and disconnection processes. Depending on whether one considers the binder material a permanent part of the robot module or not, this connection method can be considered welding or soldering. Because it is reversible, a feature not normally present in welded connections, we chose the terminology "soldering connector".

III. COMPONENT SELECTION

The primary components of a thermally actuated soldering connector are the solder and heating elements. Those are held by a carrier or substrate, to which the solder must be attached using a suitable method of application.

A. Solder

For the reasons outlined in Section II the power consumption of the connector should be as low as possible. When phase-changing binder materials are used, the melting point of the binder material determines the power requirements. If the melting point of the material is below the normal operating temperature of the modules to be joined, for example water when operating at room temperature [14], constant power input for cooling is required to persist the connection. It is therefore beneficial to select a material with melting point above the operating temperature, resulting in a connector that only requires power when forming or breaking connections by melting the binder. At the same time it should be as low as possible to minimize the power needed to heat to the melting point, which is defined by the binder material's specific heat c and the mass to be melted m :

$$P = \frac{cm}{t} \Delta T \quad (1)$$

Here, P is the required power, t the time of heating, and ΔT the difference in temperature between operating temperature and binder melting temperature in °C. This does, however, not

TABLE I
MELTING POINTS FOR A SELECTION OF LOW MELTING POINT METALS

Composition (by weight) or Common Name	Melting Point (°C)
Mercury	-39
68 % Ga, 22 % In, 10 % Sn [‡] (GalInStan)	-19
GaInSn alloys [†]	< 30
Ga	30
BiPbInSnCd alloys	> 43
51 % In, 32.5 % Bi, 16.5 % Sn (Field's Alloy) [‡]	62
50 % Bi, 26.7 % Pb, 13.3 % Sn, 10 % Cd (Wood's Alloy) [‡]	70
66 % In, 34 % Bi	72
69 % Bi, 26 % In, 17 % Tn	72
63 % Sn, 37 % Pb [‡] (Electronics Solder)	183

[†] Exhibits supercooling. [‡] Eutectic.

account for convective heat loss to the environment during the heating process:

$$\frac{dQ}{dt} = -hA(T(t) - T_{amb}) \quad (2)$$

where h is the heat transfer coefficient, $T(t)$ the momentary solder temperature, and T_{amb} the ambient temperature. It follows that in order to melt the solder, power input must exceed the convective heat loss at the melting temperature. Convective heat loss to atmosphere is relatively small when operating in air, but is an important consideration for applications where the modular robot operates submerged in liquids like those previously presented by our group [15]–[17]. In addition, the higher the power input the shorter the time to heat the substance to its melting point, which equates to a faster connector actuation for our application.

The most common solder for electronics applications is 63 % Sn, 37 % Pb. While this solder has been successfully used as a thermally activated locking mechanism for robotic joints [18], its melting temperature of 180 °C is high compared to other low melting point solder materials, a selection of which is listed in Table I. In addition, care must be taken to not unintentionally disassemble electronic circuits inside the robot, when the connector is heated to the solder melting temperature, also suggesting lower melting point binder materials.

When seeking candidate materials two additional criteria apply besides the melting temperature. First, a non-hazardous material is desirable. Alloys containing Mercury or Cadmium do not meet this requirement due to their known health effects. Second, it is desirable for the solder to have a eutectic alloy composition, meaning that all components the alloy melt at a single temperature. Of the materials listed in Table I, 51 % In, 32.5 % Bi, 16.5 % Sn alloy is the lowest melting point (62 °C) material that meets both requirements. It is therefore chosen as the binder material for the soldering connector. This metal is also known under the name Field's Alloy, after Simon Quellen Field who popularized its use.

B. Resistive Heater

Peltier elements and resistive heaters are two component classes suitable as heater. Peltier elements have the benefit of cooling under reverse polarity, which would reduce the time to connect in a soldering connector, but are more costly and not readily available in form factors suitable for automated PCB assembly. Therefore, we chose resistors as source of heat for melting Field's Alloy in the soldering connector, and rely on passive cooling during solder solidification.

The objective of generating enough heat to melt the connector's Field's Alloy in as short a time as possible is fundamentally framed by Ohm's law and the electric power converted to heat in a resistor $P = V^2 R^{-1}$ which is externally limited by the power supply. For our reference design, we assumed a P_{max} of 2.0 W, which is a typical discharge rate for rechargeable batteries at the scale of modular robot modules. The heating process is open loop.

In selecting a specific surface mount resistor, the maximal heat transfer rate from the resistive element to the terminals is the critical specification. The maximal power rating of the resistor is usually quoted as a proxy for heat transfer rate. If the resistor absorbs more power than it can reject as heat into the environment, the internal temperature rises and the resistor will fail. One might consider using specialty resistors for high power applications as heaters, but their non-standard mounting and high price are contrary to our goal of high manufacturability. We found that even cheap resistors with power ratings of 0.5 W remain functional after being repeatedly subjected to small multiples of their power rating.

The choice of resistance and package size for a soldering connector depends on size and other parameters of the specific implementation. For our reference design with a total connector surface areas of approximately 6.5 cm² we chose to arrange eight 0805-sized 10 Ω resistors rated at 1.0 W each.

C. Solder Carrier

In order to act as a connector between robot modules, Field's Alloy must be applied to an exterior surface of the robot module where it can be brought into contact with a matching surface of a neighboring module to form a soldered connection. The soldering connector uses a FR4 printed circuit board (PCB) as carrier of the solder and heaters. This PCB can be embedded into the outer shell of a robot module to become part of its surface. Because no part of the module can protrude outwards beyond the mid-plane between two connectors, the heaters must be mounted on the opposite side of the connector PCB facing the module's interior.

A schematic partial side view of the assembled PCB is shown in Fig. 2(a) with the heating resistor on the top side of the PCB and Field's Alloy applied to the bottom side. Efficient heat transfer through the solder carrier is beneficial during heating to minimize energy input, and during passive cooling to aide the dispersion of heat away from the solder. The total thermal resistance of the conductive heat transfer path from the heater to the Field's Alloy can therefore be written as a

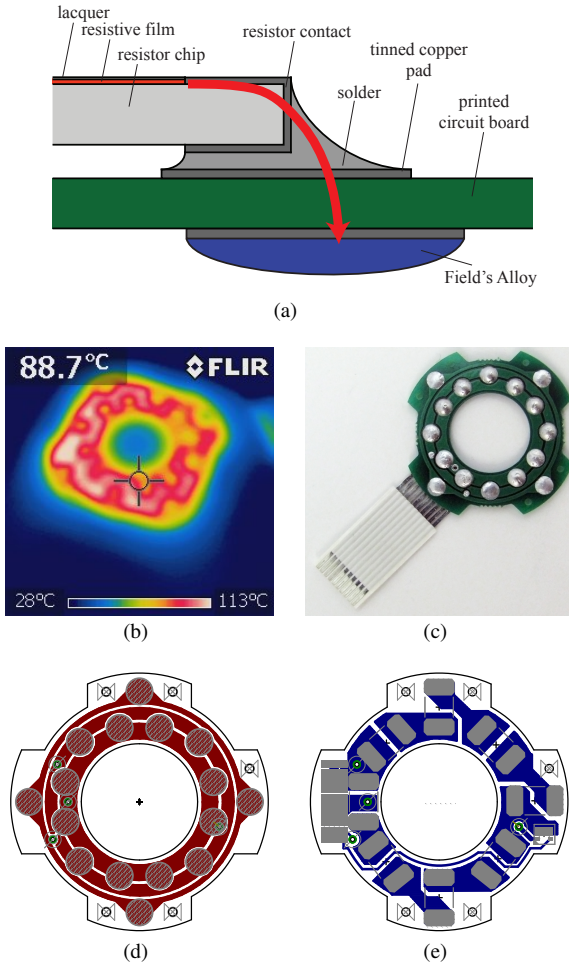


Fig. 2. Heat transfer in the soldering connector. (a) Schematic of heat transfer through a PCB with surface mount resistors and a Field's Alloy covered solder pads. (b) Thermal image of soldering connector PCB after heating continuously for 15 s at 12 V in air. (c) Top view photograph of soldering connector with flat flexible cable for connection to a module controller. (d, e) PCB drawing. Copper layer (red, blue), plated holes (green), exposed copper areas not covered by solder mask (grey).

series of thermal resistances¹:

$$R_{total} = R_{res} + R_{sol} + 2R_{cop} + R_{sub} \quad (3)$$

where the individual thermal resistances are of

- R_{res} the internal thermal resistance of the heater,
- R_{sol} the solder joint between resistor and PCB,
- R_{cop} the top and bottom copper layers of the PCB,
- R_{sub} the PCB base material, epoxy-infused fiberglass.

Of those, R_{sub} is the lowest thermal resistance due to the low thermal conductivity of epoxy-infused fiberglass ($0.16 \text{ W m}^{-1} \text{ K}^{-1}$ [21]). This makes improving the heat transfer through the PCB substrate the most effective way to reduce R_{total} . A simple way to reduce the thermal resistance of the substrate is to reduce its thickness. For our implementation of the soldering connector we chose 0.8 mm thickness substrate,

¹This representation is adapted from the more detailed characterizations of heat transfer in surface mount components by Mauney [19] and Vishay Intertechnology, Inc [20].

TABLE II
SELECTED PRINTED CIRCUIT BOARD DESIGN PARAMETERS

Design Parameter	Selection Considerations	Reference Impl.
Substrate Thickness	As thin as permitted by stiffness requirements	0.8 mm
Copper Weight	As high as possible	2.0 oz in^{-2}
Copper Coverage	As high as possible	approx. 75 %
Thermal vias	Where possible given circuit design	none
Solder Selection	High thermal conductivity is preferred	63 % Sn, 37 % Pb

a trade off between reducing thermal resistance and ensuring sufficient mechanical strength. If power and information transmission are not desired from the connector, plated holes connecting the two outer copper layers of the PCB can be used to create low thermal resistance direct metallic connections between the heating resistors and solder. A possible direction of further work not yet explored by us is the addition of internal copper layers to the PCB to increase the average thermal conductivity of the PCB. This improvement would likely be counteracted by an increased number of material interfaces; it would also increase the manufacturing cost of the connector.

The cross-sectional area of the substrate through which heat is transferred can be maximized by placing the maximal volume of copper on both top and bottom side of the PCB, while retaining electrical validity of the resulting circuit. Additionally, this decreases the thermal resistance R_{cop} of the copper layers on either side of the PCB. However, increasing the surface area of the PCB beyond what is necessary to accommodate the connector pads is not desirable because larger copper pads yield a larger heat capacity, resulting in slower heating time and facilitating heat loss to the environment. Fig. 2(d) and 2(e) show the copper layer of the reference implementation PCB with approximately three quarter of the surface area covered with copper. The thermal resistance of the copper layer itself, R_{cop} , is further reduced by choosing a high copper weight of 2.0 oz in^{-2} , equating to approximately $70 \mu\text{m}$ thickness.

R_{res} is minimized by choosing a resistor with large power rating as discussed above. The thermal conductivity k_{th} of 63 % Sn, 37 % Pb solder is quoted as $51 \text{ W m}^{-1} \text{ K}^{-1}$ [21], which is significantly higher than k_{th} for all other materials in the assembly, but R_{sol} can be reduced further by choosing higher thermal conductivity solders such as 96.5 % Sn, 3.5 % Ag ($k_{th} = 78 \text{ W m}^{-1} \text{ K}^{-1}$).

Table II summarizes which PCB design parameters can be optimized for heat transfer and specifies the values selected for our reference implementation. Fig. 2(c) shows the reference implementation of the soldering connector PCB. Fig. 2(b) validates that after 15 s of heating in air, the surface temperature of the solder reaches 70 °C to 110 °C.

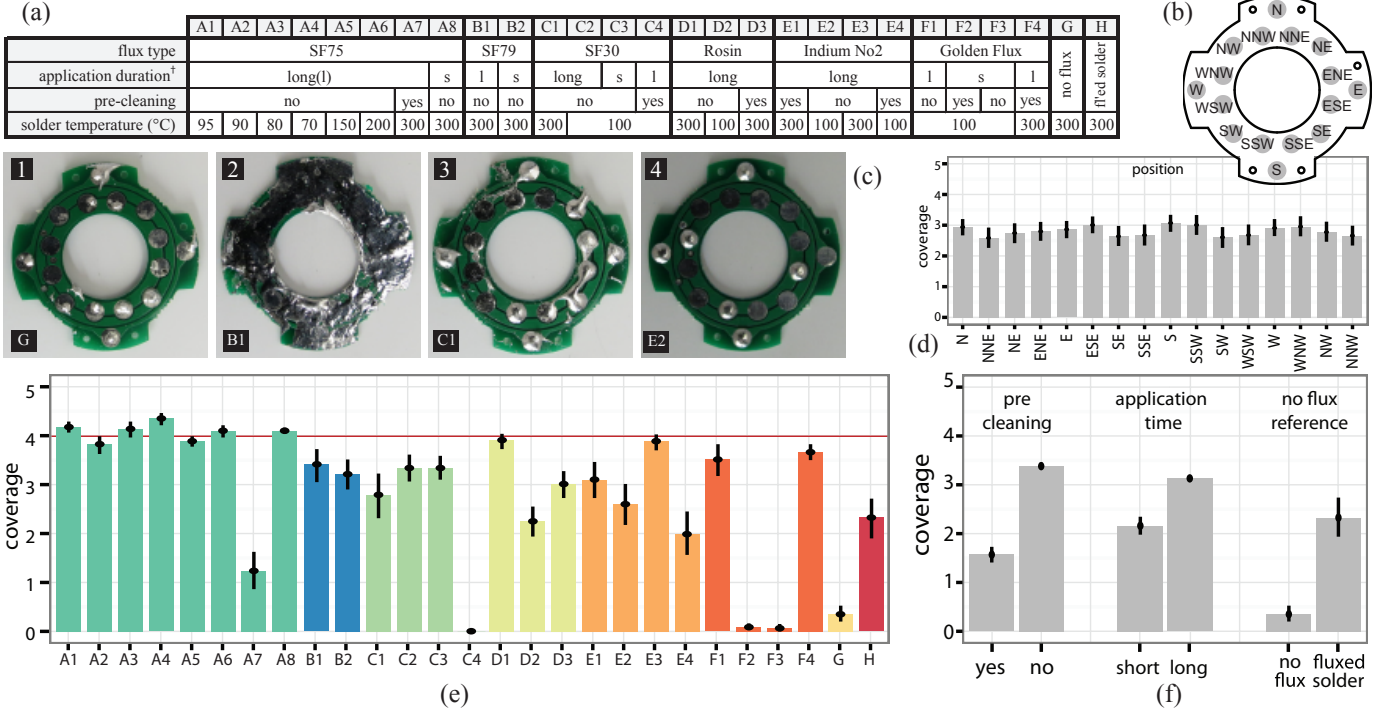


Fig. 3. Flux selection. (a) 25 experiments were conducted to select a suitable flux and process parameters for Field's Alloy application to the connector PCB. In addition, experiments G and H are control experiments with no flux and flux application to the solder respectively. For each experiment, five PCBs were manufactured and the solder coverage on each exposed copper pad was manually classified on a scale of 0 to 5. (b) The naming convention for the location of PCB copper pads used in (d) for an analysis of solder coverage quality aggregated across all experiments by location. (c) Selected photographs of results. (c1) Partial solder coverage on some pads only, (c2) solder adhesion to the entire PCB surface including solder mask, (c3) excess solder pickup resulting in short circuits between different solder pads, (c4) good solder coverage on all PCB pads. (e) Solder coverage results aggregated over five PCBs per experiment and all PCB copper pads per connector. (f) Solder coverage results aggregated by pre-cleaning and application time process parameters over experiments A1 to 8, compared to reference experiments G and H. – † Application duration: short (s) = 10 s, long (l) = 30 s.

D. Other PCB Design Considerations

In addition to facilitating heat transfer, the solder carrier PCB serves several other functions that impose design requirements.

Its function as part of the module exterior require mechanical strength that limits how thin the PCB can be, and the shape of the PCB must accommodate for other module components requiring surface area on the module surface. For example, the need to fasten the connector into the module necessitates PCB area for applying adhesives or placing mounting holes. The PCB in the reference implementation contains five countersunk holes for flat heat miniature self-tapping mounting screws.

Depending on the design of the robot module in which the soldering connector is to be used, electrical connections between the connector PCBs and another component of the module, for example a central controller PCB, are required. This wired connection is the source of power for heaters, power to be transferred through the soldering connector, and signals to be transferred through the soldering connector. Because the power that can be safely transferred through one strand of cable or one connector pin is limited and the space for terminating cable or connectors on the connector PCB is small, it is desirable to keep the number of distinct voltage levels and signals connected to each soldering connector at a minimum. For this reason, we chose the power supply voltage of our modular robot reference implementation to be equal to the

operating voltage of the soldering connector; this way only one pair of supply and ground voltages needs to be connected to each soldering connector, in addition to the signals. However, because the soldering connector's heaters must be controlled, an on-board heater switch on the soldering connector is required. A N-channel MOSFET device controlled by a 5 V signal from the main module controller can serve this purpose.

The size and arrangement of connector pads on the PCB affects the connector's tolerance to rotational and translational misalignment with the maximal tolerated misalignment between adjacent connectors proportional to the smallest distance between connector pads on the PCB. Our implementation of the connector is not optimized for tolerance to misalignment. When adjusting pad sizes, it is advisable for all pads to have the same radius. Because the contact angle of the Field's Alloy on each pad is approximately the same for all pads, smaller pads have a lower buildup of Field's Alloy which can prevent them from forming soldered connections.

Finally, with scalability towards mass manufacturing in mind, design for manufacturing (DFM) principles must be considered. Some design parameters such as copper thickness are constrained by equipment or supplier capabilities. Standard DFM techniques such as PCB panelization and sacrificial work holding features help reduce fabrication cost.

TABLE III
SELECTION OF FLUXES

Manufacturer	Product Name	Activation Temp. (°C)	Cleaning
Kapp	Golden	175 – 280	warm water
MG Chemicals	Rosin Flux	90 – 205	alc. acetate mix
Indium Corp	Indalloy Fl. #2	100 – 371	warm water
Superflux	No 30	95 – 315	warm water
Superflux	No 75	95 – 345	warm water
Superflux	No 79	95 – 315	warm water

E. Flux Selection

Undesirable properties of Field's Alloy are its high surface tension and low reactivity with other metals. Without pre-treatment of the PCB pads it is not possible to apply Field's Alloy to the carrier PCB. This was confirmed by our unsuccessful attempts to apply Field's Alloy using soldering iron and baking. In electronics assembly, flux is commonly used to prepare metal surfaces for solder application. Indeed, using Radioshack® rosin flux results in partial coverage of solder pads with Field's Alloy. Selection of a flux for optimal adhesion and solder coverage is usually based on empirical data. For the combination of Field's Alloy and tinned PCB pads we performed this selection experimentally.

The process of flux application normally consists of four steps:

- 1) Application of the flux to solder surface
- 2) Activation of the flux by heating
- 3) Pre-cleaning of excess flux from solder surface
- 4) Solder application
- 5) Post-cleaning of flux residue from solder surface

Based on exploratory experiments we determined that dipping a PCB surface into a vat of molten solder directly after flux application, that is without a separate flux activation step, can lead to complete solder coverage on the solder pads. A dipping process is more efficient than alternatives that involve solder deposition onto each solder pad separately.

To find a suitable flux and process parameters, a candidate selection of six fluxes, listed in Tab. III, and parameters were tested in a series of experiments. Fig. 3(a) lists the choice of flux, activation time, omission of pre-cleaning, and solder temperature, for 25 experiments, each consisting of the manufacturing of five identical connector PCBs. For each PCB, flux was applied to the tinned copper pads using a cotton swab, followed by waiting for the specified application time at room temperature. Subsequently the PCB was either cleaned or not (depending on the experiment), and dipped upside-down into a bath of molten solder at the temperature specified in Fig. 3(a). In addition, two control experiments were performed. One set of PCBs with no flux application, and a second where flux is applied to the surface of the heated solder vat instead of the connector PCB. The latter was to investigate the effect of pre-treating the solder surface where visible buildup and oxidation occurs.

To analyze the results quantitatively, the coverage of each

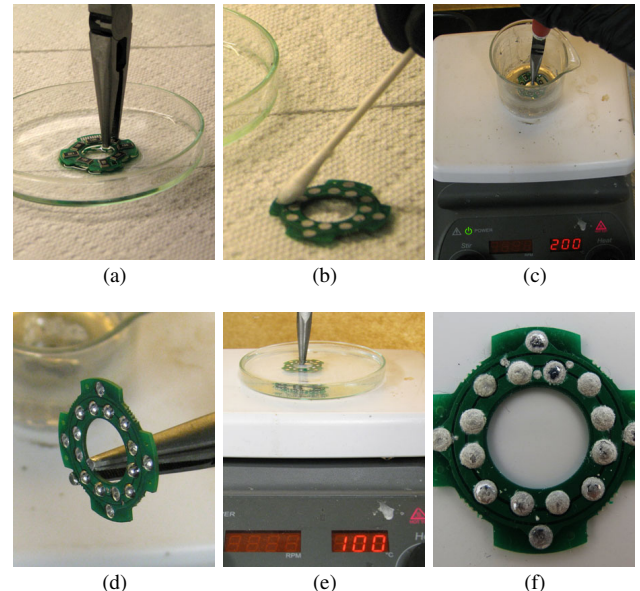


Fig. 4. Method for Field's Alloy application to connector PCB. Apply Superiorflux No 75 by dipping (a) or brushing (b). Flux activation for 30 s. Dip into Field's Alloy vat at 150 °C to 200 °C (c), resulting in solder coverage on each pad (d). Subsequently clean in warm water (e). If the cleaning step is omitted, corrosion (f) will occur.

PCB pad (see Fig. 3(b) for naming convention) is classified manually on a scale from 0 to 5, where 0 to 4 represent no solder coverage to full coverage and 5 stands for excess solder pickup on the pad. Fig. 3(c) displays a selection of results ranging from partial coverage on few pads when no flux is used (Fig. 3(c1)) to good coverage on all pads when Superiorflux® No 75 (SF75) is used without pre-cleaning (Fig. 3(c4)).

It is clear from the result in Fig. 3(e) that the use of any type of flux yields results superior to not using flux (experiment G). Of the selected fluxes, SF75 reliably results in the best solder pad coverage (experiments A1-A8) unless pre-cleaning is performed (experiment A7). The parameters pre-cleaning and flux application time are considered in isolation in Fig. 3(f). Omitting pre-cleaning and waiting for the longer period of application time results in improved solder pickup on the PCB pads. Solder temperature surprisingly does not have a significant effect on the solder coverage.

Besides incomplete solder coverage, two other error modes occur. Some parameter sets result in solder attraction to non-metallic surface sections of the PCB instead of the exposed copper sections (Fig. 3(c2)). Some parameter sets result in buildup of large amounts of solder on individual pads leading to short circuits between distinct pads (Fig. 3(c3)).

Finally, it was of concern to determine whether the placement of pads has an effect on the reliability of solder coverage. Fig. 3(d) shows the aggregate values of solder coverage for each pad location over all experiments. No significant difference between pad locations was found.

F. Solder Application Method

Based on the findings above, Fig. 4 illustrates the steps taken to apply Field's Alloy to a connector PCB. First, flux

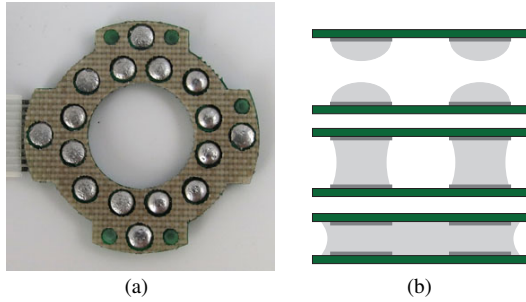


Fig. 5. Connector spacer. (a) Top view photograph of soldering connector with adhesive backed fiberglass spacer attached. (b) Effect of spacing on the connection formed with the soldering connector. If spaced too far apart, Field's Alloy from adjacent connectors will not touch and no connection is formed. Under optimal spacing, the Field's Alloy on all adjacent connectors' pads forms soldered connections. Too small spacing between adjacent connectors results in Field's Alloy spilling over the connector pad and potentially short circuits across multiple pads.

of type SF75 is applied by dipping (Fig. 4(a)) or using a cotton swab (Fig. 4(b)). After a 30 s wait the PCB is briefly dipped into Field's Alloy at approximately 150 °C to 200 °C (Fig. 4(c)), resulting in Field's Alloy to be applied to the PCB pads (Fig. 4(d)). Mild sputtering of flux can occur during this step as the flux is activated only once it is already in contact with the Field's Alloy. Finally, the flux residue is cleaned with warm water (Fig. 4(e)).

It is essential that the final cleaning step is not omitted as otherwise corrosion will occur on the soldering connector after several weeks. Fig. 4(f) shows an example of a soldering connector PCB for which the flux cleaning step was omitted with a thin layer of white corroded material that prevents soldered connections from forming.

G. Connector Spacing

The spacing between two adjacent connectors is critical for forming a functioning electrical connection between the two connectors (Fig. 5(b)). If the spacing is too large no connection is formed at all, but if the spacing is too low Field's Alloy forms unintentional connections or short circuits between neighboring pads. In order to ensure sufficient spacing between adjacent connectors, the module shell of our reference implementation is designed to result in a minimal gap of 1.2 mm between PCB surfaces when the module shells touch. In addition, an adhesive backed, PTFE-coated fiberglass film spacer is attached to the exterior facing side of the connector PCB as shown in Fig. 5(a). The film is laser cut to equal the solder mask layer of the PCB in shape. This spacer helps enforce spacing between adjacent connectors, acts as a barrier to prevent Field's Alloy spills between distinct contacts, and its PTFE coating provides a non-stick outward facing surface.

IV. EXPERIMENTAL VALIDATION

The soldering connector satisfies several of the requirements for connectors in self-reconfiguring modular robots by virtue of its design. The connector is genderless and the use of a conductive solder on a PCB substrate makes it suitable for transmitting signals and power. Further, soldering connectors

are four-fold rotationally symmetric making them orientation-invariant in a cubic lattice. Several other requirements are not as readily met and require further investigation. The following sections describe experiments carried out to evaluate the tensile strength and the durability of the soldering connector.

A. Tensile Test

The tensile strength of the connection between two modules in a modular robot directly affects the strength of the entire structure. Even though it is difficult to predict the exact forces and torques that might be acting on a connector during normal operation, a tensile test will give an indication of the magnitude of loads the connector can support, and is useful for comparing different connector designs.

We performed a series of 20 tensile tests of the soldering connector on the *freeLoader* tensile test apparatus, an open source instrument described by Amend et al. in [22]. Before performing the tests described in the following, the instrument was validated to record the tensile strength of aluminum to within 5 % of the specified value.

Fig. 6(a-c) show photographs of the test setup. Connector PCBs are fastened into 3D-printed² holders using miniature screws and adhesive. Specifically, the holder in the tensile test is the partial shell of the Soldercubes modular robot system described in Section V. The partial shells with embedded connector PCBs are then attached to 3D-printed adapters (Fig. 6(b)) in order to be mounted into the *freeLoader* material testing apparatus (Fig. 6(c)).

To create the connection between the two connectors that form one tensile test sample, both were manually placed on top of each other and both were supplied with the appropriate voltage and control signal to activate the heaters until a temperature of 90 °C was measured on the heater surface using a thermal imaging camera. At this temperature the Field's Alloy is reliably molten throughout, ensuring repeatability in the tensile test setup. After heating to form a connection the pair of joined connector PCBs were let stand to cool for five minutes and until the heater surface temperature was confirmed to be below 35 °C. Subsequently, the pair was mounted into the tensile testing machine and the tensile test started.

Ten tensile tests were carried out at a rate of elongation of 3 mm min⁻¹, and ten others at 2 mm min⁻¹ to determine if there exist time dependencies in the material behavior. A second test parameter investigated is spacing between the connector PCBs. Ten tests were performed with a spacing of 1.2 mm between the outward facing surface of the connected PCBs, and ten tests performed with connector holders that add a 0.3 mm standoff resulting in a total gap of 1.8 mm. Four test batches with five tests each were performed covering each permutation of the two test parameters. Out of those, one test was excluded from the result analysis because the adapter jig failed. Table IV shows the association between batches and test parameters.

²All 3D-printed components used for experiments and demonstrations in this paper are fabricated on an Objet Connex500 3D-printer in high quality print mode using Objet Fullcure720 material.

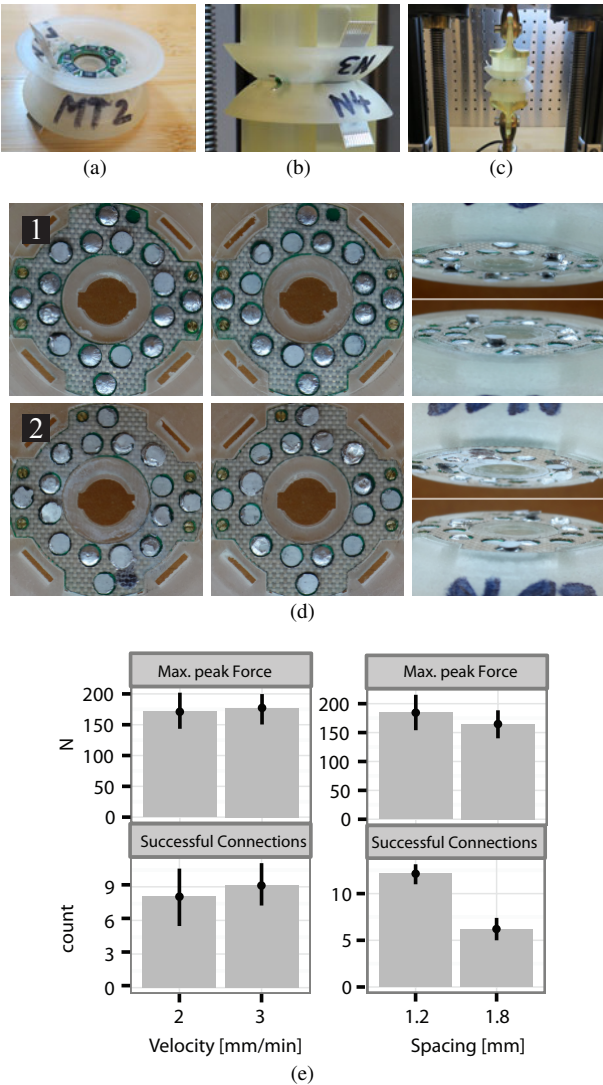


Fig. 6. Tensile test. (a) Connector PCBs are inserted into partial shells of robot modules and connected. (b) The partial module shells with attached connector PCBs are attached to 3D-printed adapter jigs. (c) Using the jigs, the pairs of connected connector PCBs are mounted in the freeLoader material testing apparatus. (d) The number of successful solder joints per connection varies and can be determined by inspecting the connector PCBs for fracture surfaces after the tensile test. (d1) is a pair of connectors with only five solder joints showing signs of successful solder joints, while for the pair in (d2) all solder joints have been formed. (e) Results for force at failure and number of fractured solder joints for all experiments aggregated by elongation rate. (f) Ditto, aggregated by initial connector PCB spacing.

Results are presented in terms of force at failure, as opposed to stress, because not all of the redundant connector pads always form a connection. Thus we do not know the surface area of the connection and stress cannot be calculated. In addition, the number of fractured connections is recorded. Fractured connections are those where a fracture surface is clearly visible on the connector pad or where the copper pad was disconnected from one of the PCBs during the failure of the connection. Connector pads that show neither of these features did not form a soldered connection during the connection process, and did therefore not carry any load. Fig. 6(d) shows one pair of connectors that features only five

TABLE IV
TENSILE TEST BATCHES AND TEST PARAMETERS

Batch	Elongation Rate	PCB Spacing
Batch 1	3 mm s^{-1}	1.2 mm
Batch 2	3 mm s^{-1}	1.8 mm
Batch 3	2 mm s^{-1}	1.2 mm
Batch 4	2 mm s^{-1}	1.8 mm

fractured connections after the tensile test (top), and one pair where all 16 connections were soldered (bottom).

The average maximal tensile force at failure is found to be 173 N with a standard deviation of 46.4 N. Fig. 6(e) and 6(f) aggregate results from all tests by elongation rate and connector spacing respectively. Grouping the results by elongation rate does not show any statistically significant difference suggesting that there is no time dependence in the failure modes observed. Grouping by initial spacing between the two connector PCBs does, however show a significant difference in the observed metrics. Most notably, the number of pads forming a connection with their counterparts on the other connector is only 50 % of the value found for the smaller spacing. Surprisingly, this does not cause the force at failure to be reduced by the same factor, suggesting that in all cases only a small number of individual solder joints contribute to the ability of the soldered connection to support loads.

B. Durability Test

To evaluate the durability of the soldering connector, repeated connection-disconnection cycles were performed in an automated experiment using a CRS A465 robot arm. The test setup, shown in Fig. 7, consists of a 3D-printed partial module shell mounted to the robot arm in place of an end effector, and a second similar shell mounted to the work surface. Connector PCBs are inserted into both partial shells using adhesive and miniature screws to resemble Soldercubes modules. Both connectors are mounted on a slider that allows for travel in the z-axis direction only. The arm mounted connector is spring loaded to simulate the elasticity inherent to a system of 3D-printed modules when compared to the rigidity of the robot arm.

The connectors in the test are electrically connected in a fashion identical to connectors in a complete robot system. Both connectors are supplied 12 V to power the soldering connector's heaters. The 5 V control line which controls the soldering connector's heaters is wired to a digital output of the robot arm's programmable logic controller.

The correctness of each soldered connection cycle is validated by applying the supply voltage and a control signal at the arm mounted connector and testing the voltages measured on the table mounted connector using an ArduinoTM Duemilanove microcontroller board as measurement device. Each test of the signal transmission line involves five 200 ms 5 V pulses spaced by 200 ms low periods. All five high and low levels must be detected at the receiving connector for the connection to be valid. This methodology is to detect both error modes of unconnected pairs of solder pads, and

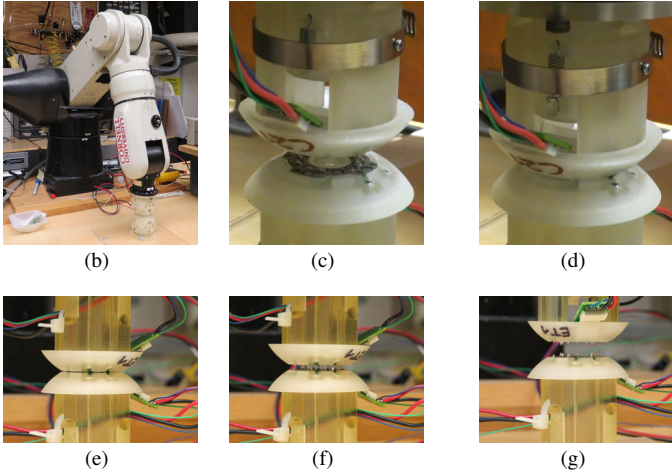
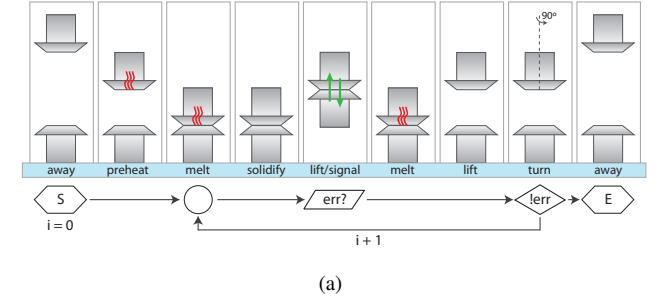


Fig. 7. Automated Repeatability Test. (a) Workflow for repeated test cycles in the repeatability test. (b) Front view photograph of CRS 456 robot arm while connecting two connectors. (c, d) Photograph of robot end effector designed to resemble soldering connector, before and while connecting, respectively. (e-g) Side view photographs of pair of connectors disconnecting.

unintentional connections between electrically distinct solder pads. Short circuits on the power supply line are detected by the associated voltage drop, while failed power supply line connections are detected as floating inputs.

The workflow for each experiment is visualized in Fig. 7(a). Starting from an *away* position the experiment begins with a short 5 s preheating phase before it enters a cycle of a user defined number of n connect-disconnect cycles. After a connection is formed, the robot arm raises to its *disconnect* position; if a soldered connection exists, the lower connector is lifted. During this state, the electrical correctness of the connection is tested.

During several preliminary tests runs, hundreds of successful cycles were regularly achieved, including one test that was terminated after 1075 cycles without failure. To make the scenario more realistic, a 90° rotation of the robot arm mounted connector after each cycle was introduced, taking into account the assumption that during normal operation in a modular robot system repeated connections between the same two connectors in the same relative orientation are unlikely. To simulate even more realistic operating conditions, a possible direction for future work is an extended experimental setup where the arm-mounted connector forms connections to several connectors in sequence.

Table V lists results of five durability tests resulting in a mean number of cycles to failure of 221 at a standard deviation

TABLE V
REPEATABILITY TEST RESULTS

Batch	Cycles to Failure	Failure Mode
# 1	70	short circuit
# 2	46	short circuit
# 3	64	short circuit
# 4	502	short circuit
# 5	422	short circuit

of 222 cycles. The only failure mode encountered were short circuits between the 12 V power supply pins and ground due to Field's Alloy spilling off the connector pads; no failure of signal transmission line was detected. A likely explanation for the unimodal failures is the placement of connector electrodes, with power and ground pads being positioned coradially.

Short circuits due to Field's Alloy spillage were of two types. In some cases Field's Alloy forms a bridge between distinct connector electrodes. This occurs when all Field's Alloy that was applied to one connector pad has transferred to the neighboring pad which then carries an excessive amount of Field's Alloy, and might be preventable if a stronger connection between the PCB pads and the Field's Alloy could be created. The second more frequent type of unintended electrical connection is between connector electrodes and other PCB features. The existence of open vias next to the connector pads is a critical flaw in our connector design. It highlights that besides the Field's Metal carrying connector pads all PCB features should be covered with solder mask.

Several additional strategies could be considered for improving durability of the connector. A reduction of the area and re-arrangement of connector pads will likely lead to a smaller probability of short circuits, but might reduce the strength of the connection. Improving the bonding of the adhesive-backed spacer described in Section III-G with the PCB could help contain the Field's Alloy on the connector pads.

V. SOLDERCUBES. A SELF-SOLDERING SELF-RECONFIGURING MODULAR ROBOT SYSTEM

Soldercubes is a self-reconfiguring modular robot system whose cube-shaped modules contain six soldering connectors, one per cube face. Soldercubes modules have one DC motor actuated rotational degree of freedom with the axis of rotation orthogonally piercing two cube faces. The module is split in such a way that one cube face, including one soldering connector, rotates relative to the remaining five. Depending on the configuration of modules in space, Soldercube can therefore operate as a chain type modular robot, or in a sparse lattice configuration. Thanks, in part, to the use of the soldering connector, Soldercubes modules are the smallest and lightest modular robot modules among comparable systems described in literature. One actuated Soldercube module weighs 120 g and occupies 75 % of a 55 mm cubic lattice cell. Our paper on the Soldercubes modular robot system [23] contains a comprehensive description of the module design.

A group of five Soldercubes were used to experimentally demonstrate the application of the soldering connector in the

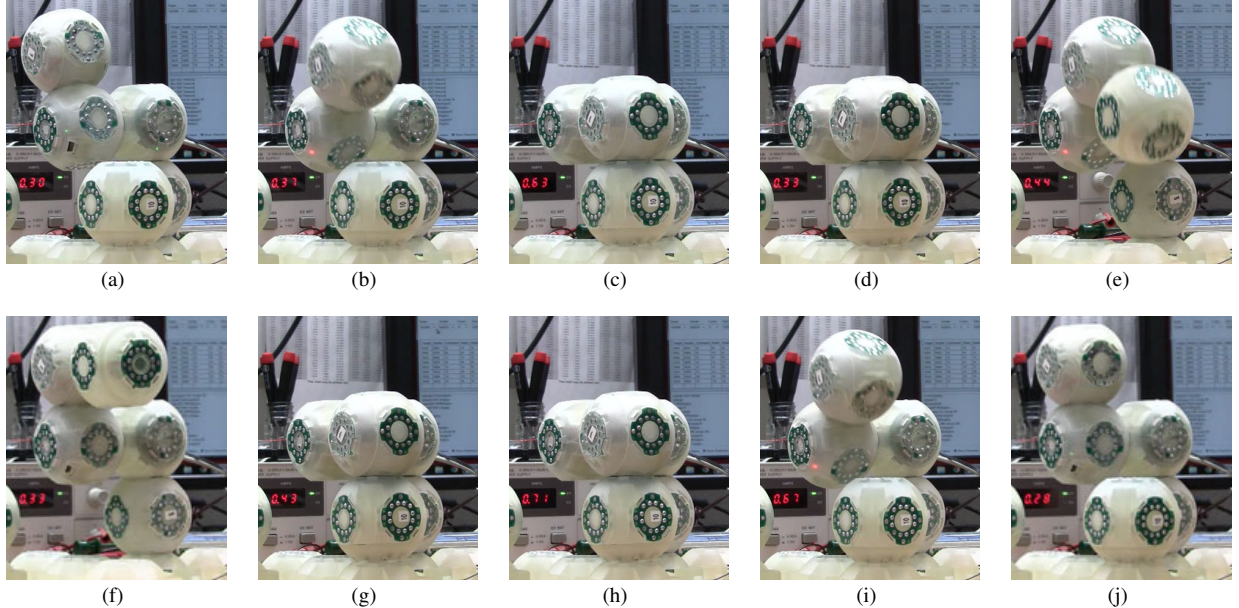


Fig. 8. A simple arm mechanism with four Soldercubes modules is used to pick up and return an individual module. The digital readout in the background shows the current consumption at 12 V. From its starting position (a) the arm mechanism lowers itself (b) until its topmost module is adjacent to the individual module. Drawing an additional 300 mA for melting the low melting point alloy for approximately 10 s (c) and subsequent cooling (d) the two adjacent modules connect and subsequently lift up together (e). From the same starting position (f) the arm lowers again (g) and the soldering connector heats (h), immediately followed by the arm moving up thereby breaking the soldered connection (i), and finally returning to the original position (j).

context of a self-reconfiguring modular robot. Four modules are arranged to form a one degree of freedom mechanism that raises or lowers a two module arm. A fifth module is placed such that it becomes adjacent to the topmost module of this arm, when the arm is lowered. Both the base of the arm mechanism and the lose module are placed on a substrate of tiles, each containing a soldering connector, that provides mechanical support and distributes power and a communications bus. The base of the arm mechanism is connected to the substrate, while the individual module only rests on a substrate tile but is not connected.

Fig. 8 depicts a sequence of photographs³ showing the arm lowering to become adjacent to the individual module, connecting to the module, lifting the module, lowering the module, disconnecting from the module, and returning to its original position. Once adjacent to each other, the module connected to the arm heats its soldering connector for approximately 10 s at an additional current consumption of approximately 300 mA followed by a 30 s cooling period. This is enough to form a mechanical and electrical connection; the newly connected module can now be addressed through the communication bus and is lifted up demonstrating the mechanical connection.

VI. REVIEW OF MODULE CONNECTION METHODS

Modular robot connectors presented in literature to date can be grouped broadly into mechanical, magnet, and binder material based connectors. In order to provide context for the development of a new modular robot connector, the existing solutions to the connection problem are reviewed in the

following paragraphs. Table VI lists connector properties for several self-reconfiguring modular robots.

A. Mechanical Connections

In a survey of connection methods for self-reconfiguring modular robots, mechanical connectors are by far the most common.

Grippers are systems where one or more actuated hooks engage a counterpart or passive structure on a neighboring module to connect. Self-reconfiguring robot systems that implement gripper mechanisms include *ATRON*, *Molecule*, *3D Unit*, *Roombots*, and *CoSMO* [30], [50]–[53]. Gripper connectors are mechanically strong and reliable enough to be used in an assembly of 100 *ATRON* modules. However, they add significant mechanical complexity to the module. Either each actuated connector requires an independent drive mechanism, or a complex clutch mechanism is required to actuate the connector independently [30]. As a result, modules with gripper connectors often have few connectors or are large.

Latched connectors are mechanical connectors where connections are formed passively but disconnection requires actuation. The *CONRO*, *Crystalline*, *I-Cubes*, *Chobie-II*, *MTRAN-III* and *Micro Unit* all slide a grooved pin into a spring loaded lock to connect, and disconnect by releasing the lock through either SMA or DC motor actuation [29], [43], [54]–[56].

A variation on the latched connector type are those where multiple pins are unlocked, and in some cases also locked, in parallel by rotating two connector plates relative to each other. This type of connector can be found in the *CONRO* and *ModRED* systems [7], [28]. *ModLock* is a connection for *ckBot* based on the same principle but manually operated and has been shown to support loads of up to 2.2 kN [57].

³A video of this experiment is available as supplementary material to this paper and on <http://creativemachines.cornell.edu/soldercubes/>.

TABLE VI
REVIEW OF CONNECTORS IN SELF-RECONFIGURING MODULAR ROBOT SYSTEMS

Name	Year	Dim	Type	Actuation	Count [†]	TS	g	P	S	Size (mm)	Weight	Ref.
CEBOT	1988	2D	latch	SMA	2 (1)	—	X	X	✓	180x90x50	1.3 kg	[24]
Metamorphic	1993	2D	active lock	DC motor	6 (3)	—	X	X	X	—	—	[25]
Polypod	1993	3D	latch	SMA	2 (2)	—	X	✓	✓	—	—	[26]
Fracta	1994	2D	electro-mag.	current	3	—	X	X	X	D:125 H:160	1.2 kg	[27]
Metamorphic2	1996	2D	active lock	DC motor	6 (3)	—	X	X	X	—	—	[25]
CONRO	1998	3D	latch	SMA	3 (1)	—	X	—	✓	L:108	115 g	[28]
Micro-Unit v1	1998	2D	latch	SMA	4 (2)	—	X	X	✓	50x50x50	50 g	[29]
Molecule	1998	3D	electro-mag.	current	10 (10)	—	X	—	—	D:102	3.2 kg	[1]
3D-Unit	1998	3D	hooks	DC motor	6 (6)	—	✓	✓	✓	L:265	7 kg	[30]
Vertical	1998	2D	perm. mag.	N/A	5 (1)	0.3 N	X	—	—	90x90x90	—	[31]
I-Cube	1999	3D	key and lock	—	2 (2)	—	X	X	✓	85x37x18	205 g	[32]
Crystalline	1999	2D	key and lock	DC motor	4 (2)	—	X	X	X	51x51x178	340 g	[11]
Micro-Unit v2	1999	2D	latch	SMA	4 (2)	—	X	X	✓	20x20x30	15 g	[33]
PolyBot	2000	3D	latch	SMA	2 (2)	—	✓	—	✓	50x50x50	200 g	[34]
MTRAN	2000	3D	perm. mag.	SMA	6 (3)	25 N	X	✓	✓	66x132x66	440 g	[35]
Telecubes	2002	3D	perm. mag.	SMA	6 (6)	—	✓	✓	✓	60x60x60	—	[36]
MTRAN-II	2003	3D	perm. mag.	SMA	6 (3)	—	X	✓	✓	60x120x60	400 g	[37]
Stochastic 2D	2004	2D	perm. mag.	DC motor	3 (3)	—	✓	X	X	60x60	100 g	[38]
Catoms	2005	2D	electro-mag.	current	24	—	✓	✓	X	D:44 H:40 [‡]	105 g	[39]
Stochastic 3D	2005	3D	electro-mag.	current	6 (6)	—	✓	✓	✓	100x100x100	—	[15]
Molecubes I	2005	3D	electro-mag.	current	2 (2)	—	✓	✓	✓	100x100x100	625 g	[40]
ATRON	2005	3D	hooks	DC motor	8 (4)	200 N	X	✓	X	D:11	850 g	[12]
Prog. Parts	2005	2D	perm. mag.	DC motor	3 (3)	—	✓	X	X	L:120 H:42	—	[41]
XBot	2007	2D	perm. mag.	SMA	4 (4)	—	✓	X	X	—	—	[42]
MTRAN-III	2008	3D	hooks	DC motor	6 (6)	—	X	✓	✓	65x65x130	420 g	[43]
Roombots	2010	3D	hook	DC motor	10 (2)	—	✓	X	X	220x110x110	1.4 kg	[10]
ModRED	2010	3D	latch	solenoid	2 (2)	—	✓	X	X	368x114x1190	3.17 kg	[44]
Pebbles	2010	2D	elec.-perm. mag.	current pulse	4 (4)	2.16 N	✓	X	X	12x12x12	4.0 g	[45]
M3 Express	2012	2D	perm. mag.	DC motor	3 (3)	11 N	✓	X	X	—	878 g	[46]
SMORES	2012	3D	perm. mag.	DC motor	4 (3)	60 N	✓	X	X	100x100x90	520 g	[47]
CoSMO	2013	3D	key and lock	DC motor	4 (4)	4kN	✓	✓	✓	105x105x105	1.25 kg	[48]
M-Blocks	2013	3D	perm. mag.	N/A	6 (0)	—	✓	X	X	—	—	[49]
Soldercubes	2014	3D	binder mat.	heat	6 (6)	173 N	✓	✓	✓	55x55x55	120 g	

Dim = dimensionality of system **TS** = tensile strength **g** = genderless? **P** = transmits power? **S** = transmits Signal? **✓** = yes. **X** = no. **—** = Information not found in published literature. [†] total (and actuated) degrees of freedom, [‡] Estimate from figures.

B. Magnetic Connections

Using magnetic force is a second approach frequently used for forming connections between robot modules. Magnetic module connectors can be categorized by their use of static and actuated permanent magnets, and electro-magnets.

Static permanent magnets are generally not useful for self-reconfiguring systems because disassembly of a connection without external manipulation is not possible. *M-Blocks* and *Vertical* are systems where module-internal actuation is employed to overcome a permanent magnet connection [31], [49]. A number of assembly systems, where disassembly is not an intended function, use permanent magnets, including *Programmable Parts* and *Stochastic 2D* [38], [41].

Active permanent magnet connectors are connectors in which permanent magnets are connected to mechanical actuators. A mechanism where shape memory alloy (SMA) wire is used to retract permanent magnets from the connected position is used in the first two generations of the *MTRAN* system and the *Telecubes* system [36], [37], [58]. In the *MTRAN* system, for example, the magnets provide sufficient force to support a force of 3.6 kg that is nearly counter-balanced by an

internal spring. When the SMA wire is heated it exerts a small force on the magnet, which in series with the spring force pulls the magnet away from the connector surface, resulting in disconnection. *M3Express* implements a similar connector actuated by small DC motors [46].

Systems that rely on electro-magnets as connectors, for example *Molecule*, *Molecule I*, and *Catoms* [1], [39], [40], suffer from constant power consumption while holding a connection, making the systems difficult to scale to large numbers of modules.

An alternative way to use mechanical actuation to disconnect permanent magnet connectors is to change the relative polarity of adjacent magnets. A commercial implementation of the actuated permanent magnet concept is available under the brand name Magswitch® from Magswitch Technology, Inc, and has been used in the *Miche* system [59].

Electro-permanent magnets are devices that can be switched from acting as a permanent magnet to a passive state, and vice versa, with a short current pulse. As a result, they have low power requirements similar to actuated permanent magnets but the switchability of an electromagnet. The *Pebbles* self-

disassembling system makes use of electro-permanent magnets [45]. In tensile tests the force to separate two adjacent Pebbles modules was determined as 2.16 N and each connector weighs 0.2 g [60]. This excludes the 100 μ F capacitor needed to generate the switching current pulse.

C. Connections with Binder Materials

More recently, a number of connection methods that use a phase changing binder material between connecting modules have been reported. Miyashita et al. use Peltier elements to freeze water between adjacent connector surfaces [14]. This connector requires constant power input to sustain cooling to retain the connection. Wang et al. use hot melt adhesives that require power only while heating to form or break connections [61]. Both applications are open loop without temperature feedback.

The soldering connector described in this paper similarly uses a binder material to form connections. It extends the methods using adhesives and water by providing superior mechanical strength and electrical conductivity for signal and power transfer.

VII. DISCUSSION

This paper presented a connector for self-reconfiguring systems that is significantly lighter, smaller, and easier to manufacture than most existing solutions. The connector is suitable for autonomous operation, with no external manipulation required during either connection or disconnection of adjacent modules. It is genderless, can be unilaterally actuated and is suitable to transfer power and signal. By selecting an appropriate solder, flux, and heater, a reference design sized for typical modular robot modules was developed that requires approximately 7 W for 10 s during connection or disconnection in air, and can function when submerged in non-conductive liquids such as oils and distilled water. In future work, both the heating and the passive cooling processes could be optimized through the use of temperature feedback.

What differentiates the soldering connector from other connection mechanisms for modular robots are its high manufacturability and low weight, size, and cost. The connector has no moving parts, is fully contained on a printed circuit board, contains only cheap surface mount components, and can easily be manufactured in bulk using the manufacturing method developed in this paper. The total parts cost for one connector is USD 1.97 at quantities larger than 2500⁴. Table VII qualitatively compares the soldering connector to existing connector types.

Our implementation has a total weight of 2 g per connector and thickness of less than 3 mm allowing for it to be embedded into the shell of the robot module. The tensile load supported by the connector before failure is 173 N, or approximately 8800 connector weights. This is weaker than mechanical connectors used in self-reconfiguring modular robot systems in absolute terms. However, when considered in relation to

⁴Including Field's Alloy, PCB fabrication, heating resistors, and heater switch. Excluding FFC connection cable. Pricing information from April 2014 from US vendors.

the module weight of a modular robot system, systems that integrate the soldering connector are likely to exceed thanks to the weight and volume reductions possible due to using the connector.

The electropermanent connector of the *Pebbles* system exhibits a similar strength-to-weight ratio as the soldering connector, switches connectivity faster, and requires less power to do so. However, the electropermanent connector requires costly custom fabrication and assembly and its scalability to larger connector sizes is unclear, particularly due to the high momentary power requirement that scales with connector volume [60].

One caveat of the soldering connector is its variable durability. While the mean number of 220 connection-disconnection cycles before failure is sufficient to support experiments typically carried out with modular robots today, the high variability with three out of five tests failing after less than 100 cycles is problematic for many applications. A comparison to other systems is not possible, because no durability test results have been published for other modular robot connectors. Design strategies to overcome the causes of low durability are mentioned in Section IV-B, and would likely also improve the connector's tolerance to misalignment.

Future work should be directed at exploring the design space of the soldering connector; the implementation presented here is only one reference design of our work that was focused on determining the basic materials and fabrication method. Experimentally investigating the effect of design parameters such as those listed in Table II on the connector properties would likely allow for improving durability and tolerance to misalignment. Future applications of the soldering connector will likely involve integration of the connector into larger subsystems, for example active mounts that would allow for sliding connector surfaces past each other without forming electrical connections, an operation not supported by the Soldercube system. Exploring applications in other areas of robotics and engineering might result in many application-specific variations of the soldering connector concept, including at scales orders of magnitude above and below that of our implementation.

REFERENCES

- [1] K. Kotay, D. Rus, M. Vona, and C. McGraw, "The self-reconfiguring robotic molecule," in *Proc. of the Int. Conf. on Robotics and Automation (ICRA)*, vol. 1. Louven, Belgium: IEEE, 1998, pp. 424–431.
- [2] M. Nilsson, "Essential properties of connectors for self-reconfiguring modular robots," in *Proc. of the Workshop on Reconfigurable Robots at the Int. Conf. on Robotics and Automation (ICRA)*. Seoul, South Korea: IEEE, 2001, pp. 4071–4076.
- [3] W.-m. Shen and P. M. Will, "Docking in self-reconfigurable robots," in *Proc. of the Int. Conf. on Intelligent Robots and Systems (IROS)*, vol. 2. Maui, HI, USA: IEEE/RSJ, 2001, pp. 1049–1054.
- [4] M. Yim, P. J. White, M. Park, and J. Sastra, "Modular Self-Reconfigurable Robots," in *Encyclopedia of Complexity and Systems Science*. Springer, 2009, pp. 5618–5631.
- [5] K. Stoy, D. Brandt, and D. J. Christensen, *Self-Reconfigurable Robots: An Introduction*. Cambridge, Mass: MIT Press, 2010.
- [6] R. F. Garcia, J. D. Hiller, K. Stoy, and H. Lipson, "A Vacuum-Based Bonding Mechanism for Modular Robotics," *IEEE Transactions on Robotics*, vol. 27, no. 5, pp. 876–890, 2011.

TABLE VII
QUALITATIVE COMPARISON OF SELECTED CONNECTION METHODS FOR SELF-RECONFIGURING SYSTEMS

	Moving Parts	Size, Weight	Strength	Switching Time	Power required for	Manufacturability
Gripper	many	large	high	~10 s	connect & disconnect	difficult
SMA Actuated Latch	many	medium	high	~1 min	disconnect only	difficult
Motor Actuated Latch	many	large	high	~10 s	disconnect only	difficult
Key and Lock	many	large	high	~10 s	connect & disconnect	difficult
SMA Actuated Perm. Magnets	many	medium	low	~1 min	disconnect only	difficult
Motor Actuated Perm. Magnets	medium	large	low	~1 s	disconnect only	difficult
Electromagnets	none	small	low	<1 s	holding	simple
Electropermanent Magnets	none	small	medium	<1 s	connect & disconnect	difficult
Frozen Water	none	small	medium	~10 s	holding	simple
Soldering Connector	none	small	medium	~30 s	connect & disconnect	simple

- [7] S. Hossain, C. A. Nelson, and P. Dasgupta, "RoGenSiD: A Rotary-plate Genderless Single-sided Docking Mechanism for Modular Self-reconfigurable Robots," in *Proc. of the Int. Design Engineering Technical Conferences and Computers and Information Engineering Conference (IDETC/CIE)*. Portland, OR: ASME, 2013.
- [8] M. Yim, W.-m. Shen, B. Salemi, D. Rus, M. Moll, H. Lipson, E. Klavins, and G. S. Chirikjian, "Modular Self-Reconfigurable Robot Systems [Grand Challenges of Robotics]," *IEEE Robotics & Automation Magazine*, vol. 14, no. 1, pp. 43–52, 2007.
- [9] K. Kotay, "Self-reconfiguring robots: designs, algorithms, and applications," PhD, Dartmouth College, Jan. 2004. [Online]. Available: <http://dl.acm.org/citation.cfm?id=1023054>
- [10] A. Spröwitz, R. Moeckel, M. Vespignani, S. Bonardi, and A. J. Ijspeert, "Roombots: A hardware perspective on 3D self-reconfiguration and locomotion with a homogeneous modular robot," *Robotics and Autonomous Systems*, vol. in press, Sep. 2013.
- [11] D. Rus and M. Vona, "A physical implementation of the self-reconfiguring crystalline robot," in *Proc. of the Int. Conf. on Robotics and Automation (ICRA)*, vol. 2. San Francisco, CA, USA: IEEE, 2000, pp. 1726–1733.
- [12] E. H. Ostergaard, K. Kassow, R. Beck, and H. H. Lund, "Design of the ATRON lattice-based self-reconfigurable robot," *Autonomous Robots*, vol. 21, no. 2, pp. 165–183, 2006.
- [13] W.-m. Shen, R. Kovac, and M. Rubenstein, "SINGO: A Single-End-Operative and Genderless Connector for Self-Reconfiguration, Self-Assembly and Self-Healing," in *Int. Conf. on Robotics and Automation (ICRA)*, 2009, pp. 1–6.
- [14] S. Miyashita, M. Hadorn, and P. E. Hotz, "Water Floating Self-assembling Agents," in *Agent and Multi-Agent Systems: Technologies and Applications*, N.-T. Nguyen, A. Grzech, R. J. Howlett, and L. C. Jain, Eds. Springer, 2007, pp. 665–674.
- [15] P. J. White, V. Zykov, J. Bongard, and H. Lipson, "Three dimensional stochastic reconfiguration of modular robots," in *Robotics: Science and Systems*, 2005, pp. 161–168.
- [16] V. Zykov and H. Lipson, "Fluidic stochastic modular robotics: Revisiting the system design," in *Proc. of the Robotics Science and Systems Workshop on Self-Reconfigurable Modular Robots*, Philadelphia, PA, USA, 2006.
- [17] J. Neubert, A. P. Cantwell, S. Constantin, M. Kalontarov, D. Erickson, and H. Lipson, "A robotic module for stochastic fluidic assembly of 3D self-reconfiguring structures," in *2010 IEEE International Conference on Robotics and Automation*. IEEE, May 2010, pp. 2479–2484.
- [18] N. Cheng, G. Ishigami, S. Hawthorne, M. Hansen, M. Telleria, R. Playter, and K. Iagnemma, "Design and analysis of a soft mobile robot composed of multiple thermally activated joints driven by a single actuator," in *2010 IEEE International Conference on Robotics and Automation*. IEEE, May 2010, pp. 5207–5212.
- [19] C. Mauney, "Thermal Considerations for Surface Mount Layouts," 2010. [Online]. Available: http://focus.ti.com/download/trng/docs/seminar/Topic_10_-_Thermal_Design_Consideration_for_Surface_Mount_Layouts.pdf
- [20] Vishay Beyschlag, "Thermal Management in Surface-Mounted Resistor Applications," Vishay Beyschlag, Tech. Rep., 2011. [Online]. Available: <http://www.vishay.com/docs/28844/tmismra.pdf>
- [21] K. Ferjutz and J. R. Davis, *ASM Handbook: Volume 6: Welding, Brazing, and Soldering*, 10th ed. Materials Park, OH: ASM, 1993.
- [22] J. R. J. Amend and H. Lipson, "freeLoader: An open source universal testing machine for high-throughput experimentation," in *Proc. of the Int. Design Engineering Technical Conferences and Computers and Information Engineering Conference (IDETC/CIE)*. Washington, DC, USA: ASME, 2011.
- [23] J. Neubert and H. Lipson, "Soldercubes: A Self-soldering Self-reconfiguring Modular Robot System," *Autonomous Robots*, no. submitted, 2014.
- [24] T. Fukuda and S. Nakagawa, "Dynamically reconfigurable robotic system," in *Proc. of the Int. Conf. on Robotics and Automation (ICRA)*. Philadelphia, PA: IEEE, 1988, pp. 1581–1586.
- [25] A. Pamecha, C.-J. Chiang, D. Stein, and G. S. Chirikjian, "Design and Implementation of Metamorphic Robots," in *Proc. of the ASME Design Engineering Technical Conference and Computers in Engineering Conference*. Irvine, CA, USA: ASME, 1996.
- [26] M. Yim, "New locomotion gaits," in *Proc. of the Int. Conf. on Robotics and Automation (ICRA)*. San Diego, CA USA: IEEE, 1994, pp. 2508–2514.
- [27] S. Murata, H. Kurokawa, and S. Kokaji, "Self-assembling machine," in *Proc. of the Int. Conf. on Robotics and Automation (ICRA)*, vol. 1. San Diego, CA, USA: IEEE, 1994, pp. 441–448.
- [28] M. Rubenstein, K. Payne, and P. Will, "Docking among independent and autonomous CONRO self-reconfigurable robots," in *Proc. of the Int. Conf. on Robotics and Automation (ICRA)*. New Orleans, LA, USA: IEEE, 2004, pp. 2877–2882.
- [29] E. Yoshida, S. Murata, S. Kokaji, A. Kamimura, K. Tomita, and H. Kurokawa, "Get back in shape! A Hardware Prototype Self-Reconfigurable Modular Microrobot that Uses Shape Memory Alloy," *IEEE Robotics & Automation Magazine*, vol. 9, no. 4, pp. 54–60, Dec. 2002.
- [30] S. Murata, H. Kurokawa, E. Yoshida, K. Tomita, and S. Kokaji, "A 3-D self-reconfigurable structure," in *Proc. of the Int. Conf. on Robotics and Automation (ICRA)*, vol. 1. Leuven, Belgium: IEEE, 1998, pp. 432–439.
- [31] K. Hosokawa, T. Tsujimori, T. Fujii, H. Kaetsu, H. Asama, Y. Kuroda, and I. Endo, "Self-organizing collective robots with morphogenesis in a vertical plane," in *Proc. of the Int. Conf. on Robotics and Automation (ICRA)*. Leuven, Belgium: IEEE, 1998, pp. 2858–2863.
- [32] C. Unsal, H. Kilicotte, and P. K. Khosla, "I(CES)-cubes: a modular self-reconfigurable bipartite robotic system," *Proc. SPIE, Sensor Fusion and Decentralized Control in Robotic Systems II*, vol. 3839, pp. 258–269, Aug. 1999.
- [33] E. Yoshida, S. Murata, S. Kokaji, K. Tomita, and H. Kurokawa, "Micro self-reconfigurable modular robot using shape memory alloy," *Journal of Robotics and Mechatronics*, vol. 13, no. 2, pp. 212–219, 2001.
- [34] M. Yim, D. Duff, and K. D. Roufas, "PolyBot: a modular reconfigurable robot," in *Proc. of the Int. Conf. on Robotics and Automation (ICRA)*, vol. 1. San Francisco, USA: IEEE, 2000, pp. 514–520.
- [35] E. Yoshida, S. Murata, A. Kamimura, and K. Tomita, "A motion planning method for a self-reconfigurable modular robot," in *Proc. of the Int. Conf. on Intelligent Robots and Systems (IROS)*. Maui, HI, USA: IEEE/RSJ, 2001, pp. 590 – 597.
- [36] J. W. Suh, S. B. Homans, and M. Yim, "Telecubes: mechanical design

- of a module for self-reconfigurable robotics," in *Proc. of the Int. Conf. on Robotics and Automation (ICRA)*, vol. 4. Washington DC, USA: IEEE, 2002, pp. 4095–4101.
- [37] H. Kurokawa, A. Kamimura, E. Yoshida, K. Tomita, S. Kokaji, and S. Murata, "M-TRAN II: Metamorphosis from a four-legged walker to a caterpillar," in *Proc. of the Int. Conf. on Intelligent Robots and Systems (IROS)*, vol. 3. Las Vegas, USA: IEEE/RSJ, 2003, pp. 2454–2459.
- [38] P. J. White, H. Lipson, and K. Kopanski, "Stochastic self-reconfigurable cellular robotics," in *Proc. of the Int. Conf. on Robotics and Automation (ICRA)*, vol. 3. New Orleans, LA, USA: IEEE, 2004, pp. 2888–2893.
- [39] J. D. Campbell, P. Pillai, and S. C. Goldstein, "The robot is the tether: active, adaptive power routing modular robots with unary inter-robot connectors," in *Proc. of the Int. Conf. on Intelligent Robots and Systems (IROS)*. Edmonton, Canada: IEEE/RSJ, 2005, pp. 4108–4115.
- [40] V. Zykov, E. Mytilinaios, H. Lipson, and M. Desnoyer, "Evolved and designed self-reproducing modular robotics," *IEEE Transactions on Robotics*, vol. 23, no. 2, pp. 308 – 319, 2007.
- [41] J. D. Bishop, S. Burden, E. Klavins, R. Kreisberg, W. Malone, N. Napp, and T. N. Nguyen, "Programmable parts: a demonstration of the grammatical approach to self-organization," in *Proc. of the Int. Conf. on Intelligent Robots and Systems (IROS)*. Edmonton, Canada: IEEE/RSJ, 2005, pp. 3684–3691.
- [42] P. J. White and M. Yim, "Scalable Modular Self-reconfigurable Robots Using External Actuation," in *Proc. of the Int. Conf. on Intelligent Robots and Systems (IROS)*. San Diego, CA, USA: IEEE/RSJ, 2007, pp. 2773–2778.
- [43] H. Kurokawa, K. Tomita, A. Kamimura, and S. Kokaji, "Distributed Self-Reconfiguration of M-TRAN III Modular Robotic System," *International Journal of Robotics Research*, vol. 27, no. 3-4, pp. 373–386, 2008.
- [44] P. Dasgupta, J. Baca, S. Hossain, A. Dutta, and C. A. Nelson, "Mechanical design and computational aspects for locomotion and reconfiguration of the ModRED modular robot," in *Proceedings of the 2013 international conference on Autonomous agents and multi-agent systems*. Richland, SC: International Foundation for Autonomous Agents and Multiagent Systems, 2013, pp. 1359–1360.
- [45] K. Gilpin, A. Knaian, and D. Rus, "Robot pebbles: One centimeter modules for programmable matter through self-disassembly," in *Proc. of the Int. Conf. on Robotics and Automation (ICRA)*. Anchorage, AK, USA: IEEE, May 2010, pp. 2485–2492.
- [46] K. C. Wolfe, M. S. Moses, M. D. Kutzer, and G. S. Chirikjian, "M3Express: A low-cost independently-mobile reconfigurable modular robot," in *Proc. of the Int. Conf. on Robotics and Automation (ICRA)*. Saint Paul, MN, USA: IEEE, May 2012, pp. 2704–2710.
- [47] J. Davey, N. Kwok, and M. Yim, "Emulating self-reconfigurable robots - design of the SMORES system," in *Proc. of the Int. Conf. on Intelligent Robots and Systems (IROS)*. Vilamoura, Portugal: IEEE/RSJ, Oct. 2012, pp. 4464–4469.
- [48] J. Liedke and H. Worn, "CoBoLD A bonding mechanism for modular self-reconfigurable mobile robots," in *Proc. of the Int. Conf. on Robotics and Biomimetics*. IEEE, Dec. 2011, pp. 2025–2030.
- [49] J. Romanishin, K. Gilpin, and D. Rus, "M-Blocks: Momentum-Driven, Magnetic Modular Robots," in *Proc. of the Int. Conf. on Intelligent Robots and Systems (IROS)*. Tokyo, Japan: IEEE/RSJ, 2013.
- [50] M. W. Jorgensen, E. H. Ostergaard, and H. H. Lund, "Modular ATRON: modules for a self-reconfigurable robot," in *Proc. of the Int. Conf. on Intelligent Robots and Systems (IROS)*, vol. 2. IEEE/RSJ, 2004, pp. 2068–2073.
- [51] D. Rus, Z. Butler, K. Kotay, and M. Vona, "Self-reconfiguring robots," *Communications of the ACM*, vol. 45, no. 3, pp. 39–45, Mar. 2002.
- [52] A. Sproewitz, M. Asadpour, Y. Bourquin, and A. J. Ijspeert, "An active connection mechanism for modular self-reconfigurable robotic systems based on physical latching," in *Proc. of the Int. Conf. on Robotics and Automation (ICRA)*. Pasadena, CA, USA: IEEE, May 2008, pp. 3508–3513.
- [53] J. Liedke, R. Matthias, L. Winkler, and H. Worn, "The Collective Self-reconfigurable Modular Organism (CoSMO)," in *Proc. of the IEEE/ASME International Conference on Advanced Intelligent Mechatronics*. Wollongong, Australia: IEEE, Jul. 2013, pp. 1–6.
- [54] D. Rus and M. Vona, "A basis for self-reconfiguring robots using crystal modules," in *Proc. of the Int. Conf. on Intelligent Robots and Systems (IROS)*. IEEE/RSJ, 2000, pp. 2194–2202.
- [55] M. Koseki, K. Minami, and N. Inou, "Cellular Robots Forming a Mechanical Structure," in *Distributed Autonomous Robotic Systems 6*. R. Alami, R. Chatila, and H. Asama, Eds. Springer, 2007, pp. 139–148.
- [56] C. Unsal and P. K. Khosla, "Solutions for 3D self-reconfiguration in a modular robotic system: implementation and motion planning," in *Proc. SPIE 4196, Sensor Fusion and Decentralized Control in Robotic Systems III*, vol. 4196. Boston, MA, USA: SPIE, 2000, pp. 388–401.
- [57] J. Davey, J. Sastra, M. Piccoli, and M. Yim, "ModLock: A manual connector for reconfigurable modular robots," in *Proc. of the Int. Conf. on Intelligent Robots and Systems (IROS)*. Vilamoura, Portugal: IEEE/RSJ, Oct. 2012, pp. 3217–3222.
- [58] E. Yoshida, S. Murata, A. Kamimura, K. Tomita, H. Kurokawa, and S. Kokaji, "Self-reconfigurable modular robots - hardware and software development in AIST," in *Proc. of the Int. Conf. on Intelligent Systems and Signal Processing*, vol. 1. Changsha, China: IEEE, 2003, pp. 339–346.
- [59] K. Gilpin, K. Kotay, and D. Rus, "Miche: Modular Shape Formation by Self-Dissassembly," in *Proc. of the Int. Conf. on Robotics and Automation (ICRA)*. Rome, Italy: IEEE, 2007, pp. 2241–2247.
- [60] A. N. Knaian, "Electropermanent magnetic connectors and actuators : devices and their application in programmable matter," PhD, Massachusetts Institute of Technology, 2010.
- [61] L. Wang and F. Iida, "Physical Connection and Disconnection Control Based on Hot Melt Adhesives," *IEEE/ASME Transactions on Mechatronics*, vol. 18, no. 4, pp. 1397–1409, Aug. 2013.



Jonas Neubert (M'07) received the M.Eng. degree in mechanical engineering from Imperial College London, London, UK, in 2008, and the M.Sc. and Ph.D. degrees in mechanical engineering from Cornell University, Ithaca NY, in 2012 and 2014.

He was a graduate student member of the Cornell Creative Machines Lab, Cornell University, Ithaca, NY, from 2008 to 2013. His current research interests include self-reconfiguring modular robotics, self-assembly, and lab automation.



Arne Rost received the Dipl.-Ing. degree in mechanical engineering from TU Darmstadt, Germany, in 2007. He worked at the Robot and Assistive Systems department at Fraunhofer IPA, Stuttgart, Germany, from 2007 to 2011. Since 2012 he with Festo AG & Co. KG, Esslingen, Germany. In 2013 he received his Dr.-Ing. degree in mechanical engineering from University of Stuttgart, Germany, and was a visiting Postdoc at the Creative Machines Lab, Cornell University, Ithaca, NY.



Hod Lipson (M'02) received the B.Sc. degree in mechanical engineering and the Ph.D. degree in mechanical engineering in computer-aided design and artificial intelligence in design from the Technion-Israel Institute of Technology, Haifa, Israel, in 1989 and 1998, respectively.

He is currently an Associate Professor with the Mechanical and Aerospace Engineering and Computing and Information Science Schools, Cornell University, Ithaca, NY. He was a Postdoctoral Researcher with the Department of Computer Science, Brandeis University, Waltham, MA. He was a Lecturer with the Department of Mechanical Engineering, Massachusetts Institute of Technology, Cambridge, where he was engaged in conducting research in design automation. His current research interests include computational methods to synthesize complex systems out of elementary building blocks and the application of such methods to design automation and their implication toward understanding the evolution of complexity in nature and in engineering.